# Structural Determinants of the C-terminal Helix-Kink-Helix **Motif Essential for Protein Stability and Survival Promoting Activity of DJ-1**\*S

Received for publication, October 18, 2006, and in revised form, February 28, 2007 Published, JBC Papers in Press, March 1, 2007, DOI 10.1074/jbc.M609821200

Karin Görner<sup>‡1</sup>, Eve Holtorf<sup>‡2</sup>, Jens Waak<sup>§</sup>, Thu-Trang Pham<sup>¶</sup>, Daniela M. Vogt-Weisenhorn<sup>¶</sup>, Wolfgang Wurst<sup>¶</sup>, Christian Haass<sup>‡</sup>, and Philipp J. Kahle<sup>‡§§</sup>

From the  $^{\pm}$ Laboratory of Alzheimer's and Parkinson's Disease Research, Department of Biochemistry, Ludwig Maximilians University of Munich, 80336 Munich, the  $^{\S}$ Laboratory of Functional Neurogenetics, Department of Neurodegeneration, Hertie Institute for Clinical Brain Research, 72076 Tübingen, the  $^{\P}$ Institute of Developmental Genetics, GSF-National Research Center for Environment and Health, 85764 Neuherberg, and the  $^\parallel$ Max Planck Institute of Psychiatry, 80804 Munich, Germany

Mutations in the PARK7 gene encoding DJ-1 cause autosomal recessive Parkinson disease. The most deleterious point mutation is the L166P substitution, which resides in a structure motif comprising two  $\alpha$ -helices (G and H) separated by a kink. Here we subjected the C-terminal helix-kink-helix motif to systematic site-directed mutagenesis, introducing helix-incompatible proline residues as well as conservative substitutions into the helical interface. Furthermore, we generated deletion mutants lacking the H-helix, the kink, and the entire C terminus. When transfected into neural and nonneural cell lines, steady-state levels of G-helix breaking and kink deletion mutants were dramatically lower than wildtype DJ-1. The effects of H-helix breakers were comparably smaller, and the non-helix breaking mutants only slightly destabilized DJ-1. The decreased steady-state levels were due to accelerated protein degradation involving in part the proteasome. G-helix breaking DJ-1 mutations abolished dimer formation. These structural perturbations had functional consequences on the cytoprotective activities of DJ-1. The destabilizing mutations conferred reduced cytoprotection against H<sub>2</sub>O<sub>2</sub> in transiently retransfected DJ-1 knock-out mouse embryonic fibroblasts. The loss of survival promoting activity of the DJ-1 mutants with destabilizing C-terminal mutations correlated with impaired anti-apoptotic signaling. We found that wild-type, but not mutant DJ-1 facilitated the Akt pathway and simultaneously blocked the apoptosis signal-regulating kinase 1, with which DJ-1 interacted in a redoxdependent manner. Thus, the G-helix and kink are critical

DJ-1 is the gene mutated in the PARK7 locus associated with autosomal-recessive Parkinson disease (PD)<sup>4</sup> (1). It is believed that loss of function accounts for the symptoms in DJ-1 mutation bearers, but it remains to be shown exactly what physiological role of DJ-1 is depleted in PD. Post-mortem studies on sporadic PD patients showed that DJ-1 did not accumulate in Lewy bodies, the neuropathological hallmark lesions of PD and related diseases. Rather, DJ-1 was prominently expressed in reactive astrocytes under neurodegenerative conditions, including PD (2-4), as well as in a transgenic mouse model of Lewy pathology (3). Astrocytes have a high antioxidative capacity and support adjacent neurons suffering from oxidative stress (5). Oxidative modifications of DJ-1 were found in brains of patients with PD and Alzheimer disease (2, 6). Thus, DJ-1 upregulation appears to be associated with oxidative stress in neurodegenerative brain.

Overexpression of DJ-1 conferred resistance against H<sub>2</sub>O<sub>2</sub>, 1-methyl-4-phenylpyridinium, bisphenol A, and other oxidative stressors in neuroblastoma cells (7-9). Conversely, RNA silencing (9) or targeted disruption of the DJ-1 gene (10, 11) enhanced cytotoxicity mediated by H<sub>2</sub>O<sub>2</sub>. The involvement of DJ-1 in the management of oxidative stress was confirmed at the level of whole organisms in DJ-1 knock-out (ko) mice and flies. The PD-relevant nigral dopaminergic neurons were slightly, but significantly sensitized to the toxin 1-methyl-4phenyl-1,2,3,6-tetrahydropyridine in mice with targeted disruption of the *dj-1* gene (10). Importantly, this phenotype was rescued with adenoviral delivery of wild-type [wt]DJ-1, but not [L166P]DJ-1 (10). Likewise, *Drosophila* deficient in the homolog DJ-1 $\beta$  were sensitized to H<sub>2</sub>O<sub>2</sub> toxicity and other forms of

<sup>&</sup>lt;sup>4</sup> The abbreviations used are: ASK1, apoptosis signal-regulating kinase 1; HA, hemagglutinin; ko, knock-out; LDH, lactate dehydrogenase; MEM, minimal essential medium; MEF, mouse embryonic fibroblast; mt, mutant; NEM, N-ethylmaleimide; PD, Parkinson disease; PTEN, phosphatase and tensin homologue deleted on chromosome 10; ROS, reactive oxygen species; Trx1, thioredoxin 1; wt, wild type.



determinants of the C-terminal helix-kink-helix motif, which is absolutely required for stability and the regulation of survival-promoting redox signaling of the Parkinson disease-associated protein DJ-1.

<sup>\*</sup> This work was supported by German National Genome Research Network (NGFN) grants 01GS0466 and 01GS0476, the (N)EUROPARK project funded by the European Community, Deutsche Forschungsgemeinschaft Program Project Grant SFB596 A12, the Hertie Foundation, and a collaborative research contract with Novartis Pharma Ltd. The costs of publication of this article were defrayed in part by the payment of page charges. This article must therefore be hereby marked "advertisement" in accordance with 18 U.S.C. Section 1734 solely to indicate this fact.

The on-line version of this article (available at http://www.jbc.org) contains a supplemental table.

<sup>&</sup>lt;sup>1</sup> Present address: Advalytix AG, 85649 Brunnthal, Germany.

<sup>&</sup>lt;sup>2</sup> Present address: Octagene GmbH, 82152 Martinsried, Germany.

<sup>&</sup>lt;sup>3</sup> To whom correspondence should be addressed: Laboratory of Functional Neurogenetics, Dept. of Neurodegeneration, Hertie Institute for Clinical Brain Research, University Clinics Tübingen, Otfried Müller Strasse 27, 72076 Tübingen, Germany. Tel.: 49-7071-29-81970; Fax: 49-7071-29-4620; E-mail: Philipp.Kahle@uni-tuebingen.de.

oxidative stress (12–14). *Drosophila* DJ-1 was cytoprotective by facilitating the Akt pathway via suppression of the phosphatase and tensin homologue deleted on chromosome 10 (PTEN) (14, 15). Furthermore, DJ-1 was found to interact with Daxx, thereby preventing formation of an active complex with apoptosis signal-regulating kinase 1 (ASK1) (16).

The most striking PARK7/DJ-1 mutations are a large genomic deletion removing virtually all protein-coding sequences, and the L166P point mutation (1). The L166P substitution impairs dimer formation and dramatically accelerates DJ-1 degradation (17–22). The L166P mutation is predicted to break a characteristic  $\alpha$ -helical fold in the C terminus, which is part of the DJ-1 dimer interface and distinguishes DJ-1 from structurally related proteins like the bacterial PH1704-type proteases and Hsp31-type chaperones (23-28).

To investigate the structural and functional importance of individual side chains and the overall topology of the DJ-1 C terminus, we introduced helix-breaking proline residues at selected sites within the G-helix and H-helix. As controls, we introduced helix-compatible substitutions at the same positions. Moreover, we inserted deletions into the helix-kink-helix region. We report that secondary structure perturbing mutations in the G-helix and kink specifically destabilized the DJ-1 dimer. The instable PD-associated [L166P]DJ-1 as well as our novel synthetic G-helix breaking [V169P]DJ-1 and kink deletion mutants failed to protect DJ-1 ko mouse embryonic fibroblasts (MEFs) against H<sub>2</sub>O<sub>2</sub> toxicity. Consistently, these DJ-1 mutants did not facilitate the stimulatory phosphorylation of the pro-survival kinase Akt and failed to repress ASK1. Thus, topology of the C-terminal helix-kink-helix motif is essential for protein stability and survival promoting activities of DJ-1.

#### **EXPERIMENTAL PROCEDURES**

Molecular Display—The atom coordinates of the 1.95-Å resolution crystal structure of the DJ-1 dimer (23) were downloaded from the Protein Data Bank (Protein Data Bank code 1PDW) and visualized with PyMOL.

Site-directed Mutagenesis—For the generation of C-terminal V5-tagged DJ-1 mutants, [wt]DJ-1/V5 (17) was used as template for two independent PCRs with the following primer pairs: forward mutagenesis primer (see supplementary table) and BamHI-Stop reverse primer, 5'-ATCTGGATCCGTCTT-TAAGAACAAGTGGAGCC-3', and for the second PCR reverse mutagenesis primer (see supplementary table) and NcoI forward primer, 5'-AACCATGGGAATGGCTTCCAA-AAGAGCTCTG-3'. These two PCR products were then used as templates for a PCR using NcoI forward primer (see above) and BamHI-Stop reverse primer (see above). Mutagenized PCR products were subcloned into pcDNA3.1/V5-His-TOPO (Invitrogen).

To generate N-terminal MYC-tagged DJ-1 mutants, first PCR products were also used as templates for a PCR with EcoRI forward primer, 5'-ACGAATTCGAATGGCTTCCAAAAG-AGCTCTGGT-3', and NotI reverse primer, 5'-AGCGGCCG-CGTCTTTAAGAACAAGTGGAGCC-3'. These PCR products were subcloned into pCMV-Myc (Clontech).

Kink deletions were sequentially introduced. First, an in-frame point deletion of Gly<sup>174</sup> was generated using EcoRI

forward primer and NotI reverse primer (see above) and the mutagenesis primers specified in the supplementary table. This MYC/ $[\Delta G174]$ DJ-1 construct then served as a template for deletion of codon 173 following the same strategy, yielding the double mutant MYC/[Δkink]DJ-1. All constructs were sequence confirmed (GATC, Konstanz, Germany).

Determination of Steady-state DJ-1 Levels—Human embryonic kidney HEK293 cells, rat pheochromocytoma PC12 cells, and MEFs were grown to near confluence in Dulbecco's minimal essential medium (MEM) plus 10% fetal calf serum and 1% penicillin/streptomycin. Transient transfection was performed using Lipofectamine 2000 (DNA:lipid ratio, 1:2.5) in Opti-MEM (Invitrogen). Two days after transfection, cells were lysed in 1% Triton X-100, 150 mm NaCl, 1 mm EDTA, 10 mm Tris-HCl (pH 7.5) plus Cømplete protease inhibitor mixture (Roche Diagnostics). Protein content in the lysates was determined with the Bio-Rad Protein Assay. After denaturing 15% PAGE, proteins were electroblotted onto polyvinylidene fluoride membranes (Millipore, Eschborn, Germany).

DJ-1 was detected on Western blots with mouse monoclonal antibodies against the epitope tags, anti-V5 (Invitrogen) and 9E10 anti-MYC (Developmental Studies Hybridoma Bank, University of Iowa, Iowa City, IA), or polyclonal rabbit antisera (see below). Equal loading was confirmed by reprobing blots with anti- $\alpha$ -tubulin (Sigma). Secondary antibodies used were peroxidase-conjugated anti-mouse and anti-rabbit immunoglobulins (Sigma). Immunoreactive bands were visualized by enhanced chemiluminescence (Amersham Biosciences).

Generation of DJ-1 Antisera—Rabbit polyclonal antiserum 3407 against DJ-1 protein was generated by injecting 400 µg of recombinant human full-length [wt]DJ-1/HIS, which was expressed in Escherichia coli and chromatography purified as described previously (17). Another rabbit polyclonal antiserum was generated against the extreme C-terminal peptide DJ-1 (167-189). The peptide AIVEALNGKEVAAQVKAPLVLKD was synthesized by the solid-phase method using Fmoc (N-(9fluorenyl)methoxycarbonyl) chemistry at 90% purity and validated by matrix-assisted laser desorption ionization time-offlight mass spectrometry and reverse phase high performance liquid chromatography. The peptide was then conjugated to keyhole limpet hemocyanin at the N-terminal end and used to immunize New Zealand White rabbits in a standard 90-day immunization protocol. Following enzyme-linked immunosorbent assay to determine the titer, the antibody was purified using peptide immunoaffinity chromatography.

Determination of DJ-1 mRNA—Total RNA was extracted from transfected cells with TRIzol (peQLab, Erlangen, Germany) and reverse transcribed using SuperScript II and oligo(dT) primers (Invitrogen). The resulting cDNAs were PCR-amplified using NcoI forward primer (see above) in combination with BamHI-V5 reverse primer: 5'-ATCTGGATCC-CGTAGAATCGAGACCGAGGAG-3' (V5 constructs), or EcoRI forward primer in combination with NotI reverse primer (see above) and  $\Delta GH$  mutagenesis reverse primer (see supplementary table) for MYC-tagged point mutants and deletion mutants, respectively. Amplification rates were linear at 25 cycles, as visualized on ethidium bromide-stained 1.2% agarose gels.



Real-time PCR was performed in a LightCycler (Roche). Two PCRs were performed with NcoI forward primer and BamHI-V5 reverse primer (see above) amplifying DJ-1, and two PCRs amplifying  $\beta$ -actin as standard (forward primer, 5'-CATG-GAGAAAATCTGGCACCACACC-3', and reverse primer, 5'-TGGCCATCTCTTGCTCGAAGTCC-3') using Fast Mix (Fast Start Taq DNA Polymerase, reaction buffer, MgCl<sub>2</sub>, SYBR Green I dye, and dNTP mixture). This master mixture was pipetted into a pre-cooled Light Cycler capillary and 50 ng of cDNA or H2O was added. Each capillary was sealed and centrifuged at 700  $\times$  g for 5 s, and the following program was started: preincubation, 95 °C for 10 min; amplification, 95 °C for 10 s, 57 °C for 10 s, 72 °C for 15 s (45 cycles); melting curve, denaturation 95 °C for 20°/s, annealing 65 °C for 15 s, melting 95 °C for 0.1°/s continuously; cooling, 40 °C for 30 s. Amplification curves, melting curve, and the Cp temperatures were computed (LightCycler software version 4.0).

Pulse-Chase Labeling—HEK293T cells were transiently transfected as above. One day after transfection the cells were starved in methionine/cysteine-free MEM (Sigma) plus 1% L-glutamine and 1% penicillin/streptomycin for 1 h. They were then pulsed for 3 h with 75  $\mu$ Ci/ml [ $^{35}$ S]methionine/[ $^{35}$ S]cysteine (Promix) (Amersham Biosciences), rinsed, and chased with Dulbecco's MEM (PAA, Pasching, Austria) plus 1% L-glutamine, 1 mm L-methionine, 10% fetal calf serum, and 1% penicillin/streptomycin. The cells were lysed in 1% Triton X-100, 150 mm NaCl, 2 mm EDTA, 50 mm Tris (pH 7.6) plus Cømplete protease inhibitor mixture, and immunoprecipitation was performed with monoclonal anti-V5 or anti-MYC and protein G-Sepharose (Sigma). After denaturing 15% PAGE, the gels were fixed, soaked in Amplify (Amersham Biosciences), and dried. The radiolabeled proteins were visualized on BioMax film (Kodak).

For quantification, dried gels with radiolabeled proteins were put on a white screen for 1 day. The screen was then scanned with a PhosphorImager (GE Healthcare). Metabolically labeled full-length DJ-1 bands were quantified in triplicate with the ImageQuant program. Band intensities of the 10-h time points were calculated in percentage to the DJ-1 band intensity protein at 0-h time point. Quantitative pulse-chase experiments were performed covering 10 chase times ranging from 15 s to 24 h, and half-life times were calculated by a non-linear least squares curve fit assuming a first order exponential decay rate ( $y = e^{-kt}$ ).

Proteasome Inhibition—HEK293T cells were transiently transfected with C-terminal tagged mt DJ-1 and cultured for 24 h. Then pulse-chase experiments were performed in the presence of 10  $\mu$ M MG-132 (Calbiochem), or incubated for up to 24 h with 1  $\mu$ M epoxomicin (Calbiochem) and steady-state DJ-1 levels at selected time points were determined by Western blotting with 3407 polyclonal to detect DJ-1, mouse monoclonal antibody against β-catenin (Transduction Laboratories, Lexington, KY), to measure efficiency of proteasome inhibition, and anti-β-actin (Sigma) to confirm equal loading. Both proteasome inhibitors were delivered in 0.1% dimethyl sulfoxide as vehicle.

Dimerization of DJ-1—HEK293T cells were transiently cotransfected with point mt DJ-1/V5 constructs and MYC/

[wt]DJ-1 using Lipofectamine 2000. After 30 h, cells were lysed in 1% Triton X-100, 150 mm NaCl, 2 mm EDTA, 50 mm Tris (pH 7.6) plus Cømplete protease inhibitor mixture, and immunoprecipitation was performed with monoclonal anti-V5 and protein G-Sepharose. After denaturing 15% PAGE and Western transfer, blots were sequentially probed with polyclonal anti-bodies against MYC (Santa Cruz Biotechnology, Santa Cruz, CA) and monoclonal anti-V5.

N-terminal MYC-tagged deletion mutants were co-transfected with [wt]DJ-1/V5 in HEK293T cells. After 24 h cell lysates were prepared as above and incubated for 1 h with anti-MYC agarose affinity gel (Sigma). Immunoprecipitates were subjected to denaturing 15% PAGE and Western transfer, and blots were probed with 9E10 monoclonal anti-MYC and monoclonal anti-V5.

Establishment of DJ-1-deficient MEF Cell Cultures—DJ-1 ko mice were generated using the genetrap approach (described in detail elsewhere). Briefly, genetrap ES cells (clone XE726 from Baygenomics) were generated using the genetrap vector pGT1Lxf. The vector was inserted in the intron between exons 6 and 7. This insertion is predicted to truncate the DJ-1 protein after amino acid residue 136. We verified at the mRNA level the truncation of DJ-1 and showed at the protein level that no [wt]DJ-1 protein was present (data not shown). Cells of the XE726 ES cell clone were of the OLA/SV129 strain and were used to inject into C57BL6/J blastocysts to generate chimeras, which were then mated with C57BL6/J wt mice. The heterozygote offspring was interbred to generate mt mice and wt littermate controls.

DJ-1 ko mouse embryos were dissected, heads and red organs were removed and minced in cell culture plates containing Dulbecco's MEM supplemented with 50% fetal calf serum and 1% penicillin/streptomycin. As the cultures reached stable growth, serum was gradually reduced to 10%. Then MEFs were immortalized by lipofection with 4  $\mu g$  of pMSSVLT harboring the SV40 large T antigen (kindly provided by P. Saftig, University of Kiel). After  $\sim\!50$  passages, immortalized MEFs were used in transient transfection experiments with DJ-1 constructs.

Genotyping was performed on genomic DNA extracted with the DNeasy kit (Qiagen). PCR with wt primer forward, 5'-AGGCAGTGGAGAAGTCCATC-3', and wt primer reverse, 5'-AACATACAGACCCGGGATGA-3', and mt primer reverse, 5'-CGGTACCAGACTCTCCCATC-3', amplified 475- and 230-bp products in wt and mt MEFs, respectively. In addition, Southern blot analysis of HindIII-digested genomic DNA generated 8.4- and 16-kb fragments corresponding to wt and mt MEFs, respectively (data not shown).

 $H_2O_2$  Cytotoxicity Assay—Immortalized MEF cell cultures were transfected with DJ-1 expression constructs using Lipofectamine 2000. After 24 h, 10,000 cells per well covered with poly-L-lysine (BD Biosciences) were seeded in 96-well plates. After another 24 h, cells were either treated or not with 20 μM  $H_2O_2$  for 15 h. One-half of the cells were lysed in 9% Triton, the other half was left untreated for 45 min in the incubator. Medium (50 μl) of each well was transferred into a fresh microtiter plate and 50 μl of Cyto Tox 96 substrate mixture (Promega) was added. After a 30-min incubation at room temperature in the dark, 50 μl of stop solution was added and absorption at 490



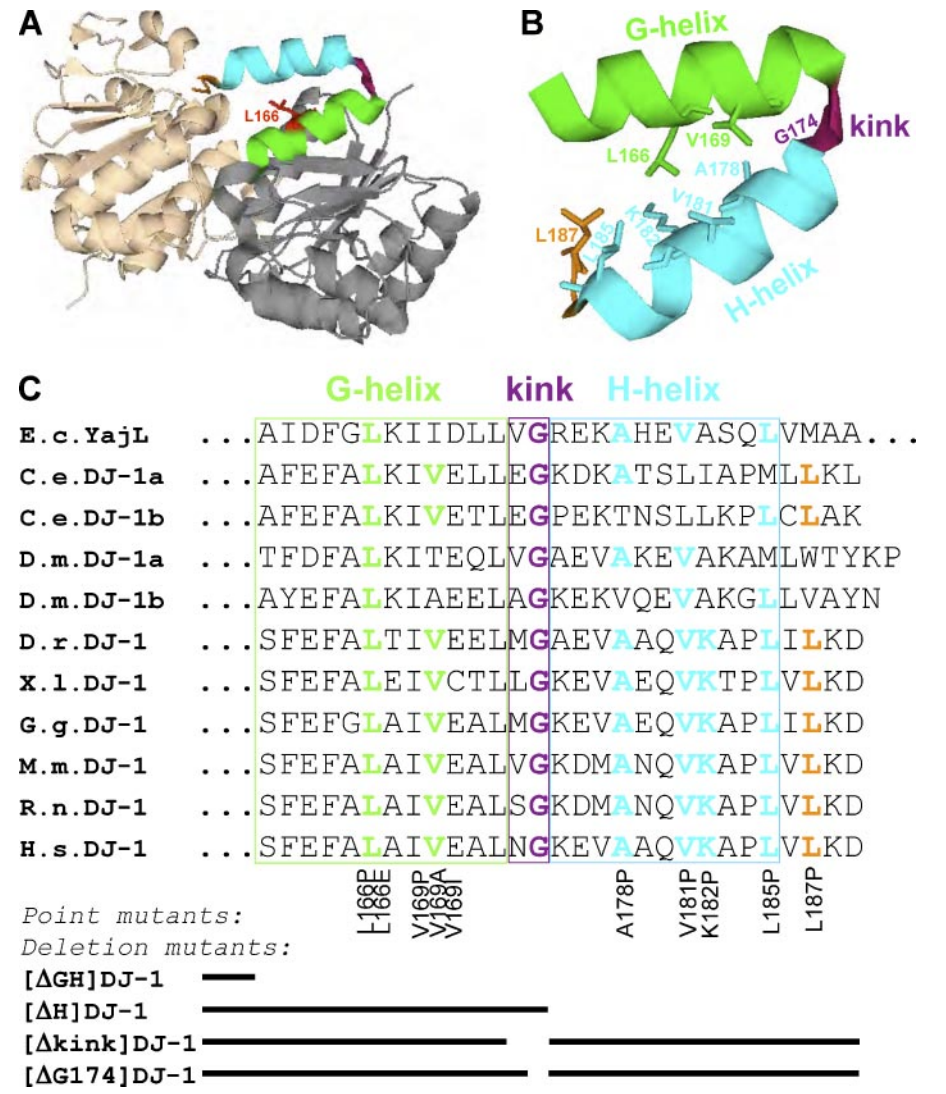


FIGURE 1. Localization of mutated residues in the C-terminal helix-kink-helix motif of DJ-1. A, the crystal structure of the DJ-1 dimer is depicted as a ribbon diagram with one homomer colored gray and the other offwhite. C-terminal secondary structure elements are colored: helix G, green; kink, purple; helix H, cyan; extreme C terminus, orange. The PD-mutated Leu<sup>166</sup> is highlighted red. B, the C terminus of DJ-1 comprises a helix-kink-helix motif with the hydrophobic side chain of Leu<sup>166</sup> in the center. Amino acid residues that were selected for site-directed mutagenesis based on structural considerations (see text for rationale) are identified. C, DJ-1 is evolutionarily conserved from mammals to bacteria; YajL from E. coli is taken as representative of prokaryotic DJ-1 sequences. Point mutated amino acid residues (bold) in helix G are highlighted green, those in helix H cyan, Glu<sup>174</sup> within the kink purple, and Leu<sup>187</sup> protruding into the helix-kink-helix orange. Deletion mutations are schematically represented by bars below.

nm measured in a photometer. Cytotoxicity was determined by calculating the lactate dehydrogenase (LDH) release into the medium divided by maximal LDH release upon cell lysis.

Measurement of Reactive Oxygen Species (ROS)—DJ-1<sup>-/-</sup> MEF cell cultures were transfected with MYC/DJ-1 expression constructs using Lipofectamine 2000. After 24 h, cells were harvested and seeded (20,000 viable, trypan blue excluding cells per well) into black microtiter plates. Another 24 h later, cells were loaded for 30 min with 100 μM dichlorodihydrofluorescein diacetate (Molecular Probes, Leiden, Netherlands) in Dulbecco's MEM plus 10% fetal calf serum. After washing, the cells were incubated for 1 h in KRH buffer (118 mm NaCl, 4.8 mm KCl, 1.2 mm MgSO<sub>4</sub>, 2.5 mm CaCl<sub>2</sub>, 5 mm glucose, 10 mm HEPES pH 7.4) with or without 200 μM diamide (Fluka, Steinheim, Germany). The amount of dichlorofluorescein generated

was determined in a fluorescence plate reader with 485 nm excitation and 525 nm emission wavelengths, respectively. Fluorescence was normalized to the protein content of the well, as determined by BCA protein assay (Pierce).

Assessment of Akt Pathway and ASK1 Activity-MEFs were transiently transfected with MYC/DJ-1 constructs using Lipofectamine 2000 and 48 h later incubated overnight in serum-free Dulbecco's MEM containing 1% bovine serum albumin. After stimulation with 500  $\mu$ M H<sub>2</sub>O<sub>2</sub> for 30 min, cells were lysed in lysis buffer (see above) plus 100 mm NaF, 1 mm NaVO<sub>3</sub>, 10 mm  $Na_4P_2O_7$ .

To determine the oxidation state of PTEN, lysates were reacted with 10 mm N-ethylmaleimide (NEM) for 15 min on ice. Samples were centrifuged for 10 min at 16,000  $\times$  g, and supernatants mixed with nonreducing Laemmli buffer. Forty μg of sample was subjected to denaturing 10% PAGE and immunoblotting using anti-PTEN (Cell Signaling, Beverly, MA). For determination of Akt phosphorylation, samples were subjected to denaturing 15% PAGE, and Western blots were sequentially probed with phospho-specific anti-[p-T308]Akt, anti-Akt (Cell Signaling), and anti- $\alpha$ -tubulin as loading controls, and 9E10 anti-MYC to measure MYC/DJ-1 expression in parallel.

To measure ASK1 activity, immunocomplex kinase assays were performed with the same lysates. Immunoprecipitation was per-

formed with ASK1 antibody (Santa Cruz Biotechnology) and protein A-Sepharose (Sigma) overnight. Immunoprecipitates were washed three times with lysis buffer and once with H<sub>2</sub>O, followed by washing with kinase buffer (Cell Signaling). Beads were resuspended in 27  $\mu$ l of kinase buffer and 1  $\mu$ l each of 10 mm ATP, 10  $\mu g/\mu l$  myelin basic protein, 10 MBq/ $\mu l$  of  $[\gamma^{-32}P]$ ATP was added. After a 20-min incubation at 37 °C, the reaction was stopped with 4× Laemmli buffer. Samples were heated at 95 °C for 5 min and loaded on two denaturing 15% polyacrylamide gels. One gel was Coomassie stained, dried, and the radioactive proteins were visualized on BioMax film. The other gel was Western blotted and probed with 3E8 monoclonal DJ-1 antibody (Stressgen, San Diego, CA).

For ASK1 co-immunoprecitations, HEK293E cells were transiently co-transfected with constructs encoding ASK1



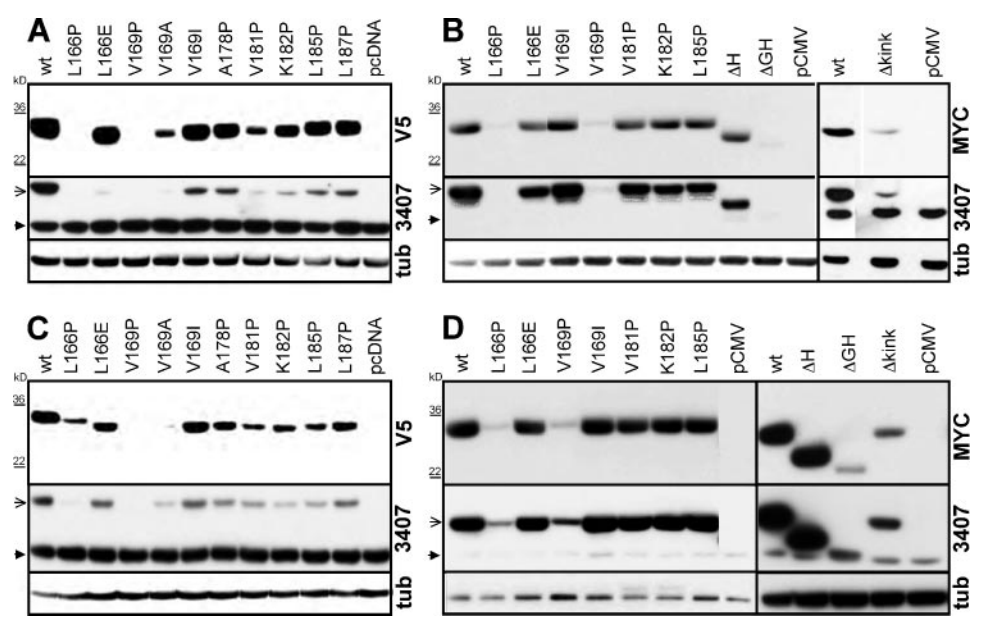


FIGURE 2. G-helix breaking and kink deletion mutations reduce steady-state expression of DJ-1 protein. PC12 (A and B) and HEK293T cells (C and D) were transiently transfected with C-terminal V5-tagged (A and C) and N-terminal MYC-tagged (B and D) DJ-1 constructs with the indicated mutations or vector alone. Steady-state DJ-1 levels in whole cell lysates were determined on Western blots probed with anti-V5 and anti-MYC, respectively (upper panels) and polyclonal antiserum 3407 against DJ-1 (middle panels). Positions of molecular weight markers are indicated to the left, open arrows denote tagged, transfected DJ-1, and filled arrows endogenous DJ-1. Equal loading was confirmed by reprobing the blots with an antibody against  $\alpha$ -tubulin (lower panels).

fused to a C-terminal hemagglutinin (HA) tag (kindly provided by H. Ichijo, University of Tokyo, Japan) and MYC/DJ-1. Two days after transfection, cells were lysed in 0.2% Nonidet P-40, 10 mm KCl, 50 mm NaCl, 1 mm EDTA, 0.5 mm EGTA, 1.5 mm MgCl<sub>2</sub>, 10% glycerol, 10 mm sodium PP<sub>i</sub>, 1 mm dithiothreitol, 50 mм HEPES (pH 7.5) plus Cømplete protease inhibitor mixture, and immunoprecipitated with monoclonal anti-HA-agarose (Sigma). Samples were electrophoresed through 4-20% Tris glycine polyacrylamide gels (Invitrogen). Corresponding Western blots were sequentially probed with polyclonal antibodies against ASK1 and human thioredoxin 1 (Trx1) (Cell Signaling), and monoclonal 9E10 anti-MYC.

#### **RESULTS**

The DJ-1 crystal structure contains a prominent C-terminal fold comprising two  $\alpha$ -helices (termed G and H) connected by a kink (Fig. 1). Both helices are well conserved (29), and in between at position 174 there is a glycine residue allowing very tight turns, which is absolutely conserved down to bacteria (Fig. 1C). The C-terminal helix-kink-helix configuration sets DJ-1 apart from the other members of this protein superfamily (30), and may therefore be an important structure and/or function determinant of the PD-associated protein DJ-1. This assumption is further emphasized by the fact that the most dramatic PD point mutation is substituting Leu<sup>166</sup> in the middle of helix G with a helix-breaking proline (Fig. 1).

To study if the deleterious effect of the L166P mutation is due to a lack of a hydrophobic side chain oriented into the helixkink-helix fold, we generated the [L166E]DJ-1 mutant. The acidic residue glutamate is well compatible with secondary structure elements, and at position 166 of DJ-1 one might even

expect some electrostatic interaction with residue Lys182 located on the opposite helix. On the other hand, to study if the L166P mutation exerts its deleterious effects by disrupting the G-helix secondary structure, we introduced a helix-incompatible proline residue one turn downstream of the PD mutant at position 166, yielding [V169P]DJ-1. The corresponding conservative mutants [V169I]DJ-1 and [V169A]DJ-1 were generated as controls.

To investigate the contribution of the H-helical part of the DJ-1 helixkink-helix motif, we systematically introduced proline residues at the positions of amino acids oriented toward the opposing G-helix, generating mutants [A178P]DJ-1, [V181P]DJ-1, [K182P]DJ-1, and [L185P]DJ-1. We also mutagenized to proline Leu<sup>187</sup>, whose side chain stretches into the helix-kink-helix motif and is engaged in hydrophobic interactions with Val<sup>181</sup>, Lys<sup>182</sup>, and Leu<sup>166</sup> (23).

Furthermore, we inserted deletions into the helix-kink-helix fold (Fig. 1C). Single deletion of the tight turn at Gly<sup>174</sup> was designed to perturb secondary structure within the kink, and double deletion of amino acids. Asn<sup>173</sup> and Gly<sup>174</sup> yielded [ $\Delta$ kink]DJ-1. Deletion of helix H and the extreme C terminus resulted in a C-terminal-truncated DJ-1 mutant lacking amino acids 175–189 ([ $\Delta$ H]DJ-1), and the entire helix-kink-helix motif was deleted in a mutant lacking amino acids 161-189 ( $[\Delta GH]DJ-1$ ).

All substitution mt DJ-1 cDNAs were cloned in-frame with a C-terminal V5 tag as described previously for [L166P]DJ-1 (17). To rule out artifacts due to the addition of a tag at the C terminus, we also cloned the DJ-1 mutants in-frame with an N-terminal MYC tag. These constructs were transiently transfected into rat pheochromocytoma PC12 cells and human embryonic kidney HEK293T cells. Two days after transfection, the steadystate levels of the DJ-1 mutants were determined on immunoblots of whole cell lysates (Fig. 2). Generally, the C-terminal V5-tagged constructs gave lower signals relative to endogenous DJ-1 than the N-terminal MYC-tagged ones, hinting to the importance of an intact C terminus of DJ-1. Compared with [wt]DJ-1, [L166P]DJ-1/V5 levels were greatly reduced and MYC/[L166P]DJ-1 was practically undetectable in both cell lines. In contrast, steady-state levels of [L166E]DJ-1 were much higher than [L166P]DJ-1, reaching almost wt levels regardless of tag or cell type (Fig. 2). Thus, the deleterious effect of the L166P mutation on DJ-1 expression seems to be due to a G-helix break rather than loss of the hydrophobic leucine side chain. Indeed, insertion of a helix-breaking proline one turn downstream abolished the protein expression of [V169P]DJ-1, whereas the conservative mutation V169I did not affect DJ-1

protein stability at all (Fig. 2). Interestingly, removal of the hydrophobic Val<sup>169</sup> side chain markedly reduced the steadystate levels of the [V169A]DJ-1/V5 mutant protein, pointing to some importance of hydrophobic contacts close to the kink.

In contrast to the dramatic effects of G-helix breaking mutations, introduction of prolines along the H-helix interface only mildly affected mt DJ-1 levels, if at all. Only [V181P]DJ-1/V5 levels were appreciably reduced in both PC12 and HEK293T cells (Fig. 2, A and C), but this effect was not observed for MYC/ [V181P]DJ-1 (Fig. 2, B and D). Mutation of the C-terminal Leu<sup>187</sup> only mildly decreased expression levels when comparing [L187P]DJ-1/V5 signals with [wt]DJ-1/V5 (Fig. 2, *A* and *C*).

The relatively small contribution of the H-helix for DJ-1 protein stability was confirmed by deletion of the H-helix and extreme C terminus, which barely reduced protein levels of MYC/ $[\Delta H]DJ$ -1 relative to MYC/[wt]DJ-1. In contrast, deletion of the entire helix-kink-helix motif abolished expression of MYC/ $[\Delta GH]DJ$ -1 in both cell lines (Fig. 2, B and D). Remarkably, we found that the kink was of critical importance for DJ-1 stability. Deletion of the kink (Asn<sup>173</sup>–Gly<sup>174</sup>) greatly reduced MYC/[Δkink]DJ-1 steady-state expression levels compared with MYC/[wt]DJ-1 (Fig. 2, B and D).

Use of 3407 polyclonal antiserum, which we raised against human recombinant DJ-1 confirmed the results of epitope tag Western probings (Fig. 2). Thus, the disappearance of the G-helix breaking point mutants [L166P]DJ-1 and [V169P]DJ-1, and the deletions MYC/ $[\Delta kink]DJ$ -1 and MYC/ $[\Delta GH]DJ$ -1 was due to loss of protein rather than limited proteolysis and cleavage of the terminal epitope tags. In conclusion, the G-helix and kink are pivotal secondary structure elements of the C-terminal helix-kink-helix motif of DJ-1, with minor contributions from the H-helix and extreme C terminus.

To determine whether the loss of steady-state expression of mt DJ-1 occurred at the mRNA level, reverse transcriptase-PCR experiments were performed. Two days after transient transfection, total RNA was extracted and reverse transcribed. Using the resulting cDNA samples as templates, semi-quantitative PCR yielded the same amounts of product for all DJ-1 mutants (Fig. 3, A and B). The effect of the most dramatic G-helix breaking mutations L166P and V169P on mRNA expression was measured more precisely by real-time PCR (Fig. 3C). The amplification curves for [L166P]DJ-1/V5 and [V169P]DJ-1/V5 were no different from [wt]DJ-1/V5. Thus, G-helix mutations appear to affect DJ-1 at the protein level.

Pulse-chase experiments with transiently transfected HEK293T cells demonstrated that [wt]DJ-1/V5 is a very stable protein with a half-life time of >24 h, whereas full-length [L166P]DJ-1/V5 was completely degraded in less than 2 h, consistent with previous reports (17, 19, 21, 22). The G-helix breaking L166P and V169P mutations had the same detrimental effect on DJ-1 protein stability (Fig. 4A). The conservative V169I did not significantly alter DJ-1 protein stability, and the less destabilized [L166E]DJ-1/V5 mutant was also not significantly different from [wt]DJ-1/V5 in pulse-chase experiments (Fig. 4A). Likewise, N-terminal-tagged MYC/[L166P]DJ-1 and MYC/[V169P]DJ-1 had greatly reduced pulse-chase signals compared with the stable MYC/[wt]DJ-1 and the control mutant proteins MYC/[L166E]DJ-1 and MYC/[V169I]DJ-1

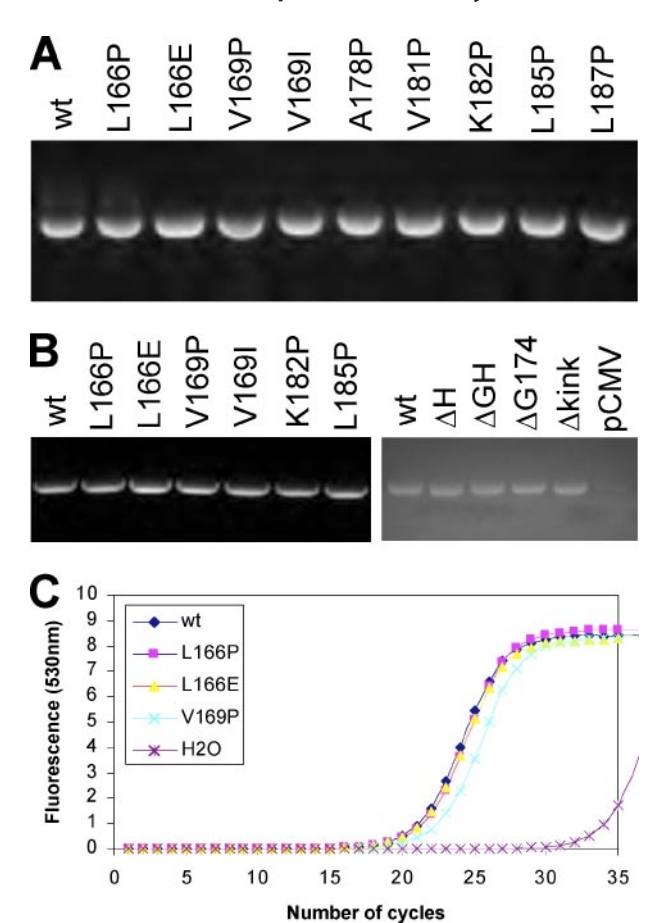


FIGURE 3. Mutagenesis at the DJ-1 C terminus does not alter mRNA levels. Total RNA was extracted from HEK293T cells transiently transfected with C-terminal V5-tagged (A and C) and N-terminal MYC-tagged (B) DJ-1 constructs with the indicated point (left panel) and deletion (right panel) mutations plus pCMV vector control (last lane). After reverse transcription, cDNA samples were amplified by PCR and subjected to agarose gel electrophoresis followed by ethidium bromide staining (A and B), or subjected to real-time PCR (C). Incorporation of the SYBR Green dye into the PCR products was plotted in the amplification curves.

(Fig. 4B). Consistent with the very low steady-state expression levels, MYC/ $[\Delta kink]DJ$ -1 showed dramatically reduced protein stability in pulse-chase experiments (Fig. 4B). In contrast, H-helix mutants only weakly altered the half-life time of the DJ-1, if at all (Fig. 4B, and results not shown). Thus, regardless of the position of short epitope tags, breaking the G-helix and perturbing the kink specifically destabilizes the DJ-1 protein.

Enhanced degradation of [L166P]DJ-1 was reported to involve the proteasome (20-22), at least in part. Consistent with our previous report (17), quantitative pulse-chase experiments showed only a small increase in half-life time of [L166P]DJ-1/V5 in the presence of the reversible inhibitor MG-132 ( $t_{1/2}$ , control, 100 min;  $t_{1/2}$ , MG-132, 112 min). Use of epoxomicin, a more specific, irreversible inhibitor of the major chymotrypic proteasome activity allowed prolonged inhibition with less toxic side effects. The long-lived endogenous DJ-1 and [wt]DJ-1/V5 did not significantly accumulate over the whole time course of epoxomicin treatment (Fig. 5). However, the highly unstable proteins [L166P]DJ-1/V5, [V169P]DJ-1/V5, and  $[\Delta GH]DJ-1/V5$  accumulated after long-term (24 h) epoxomicin treatment (Fig. 5), whereas  $\beta$ -catenin, a control protein known to

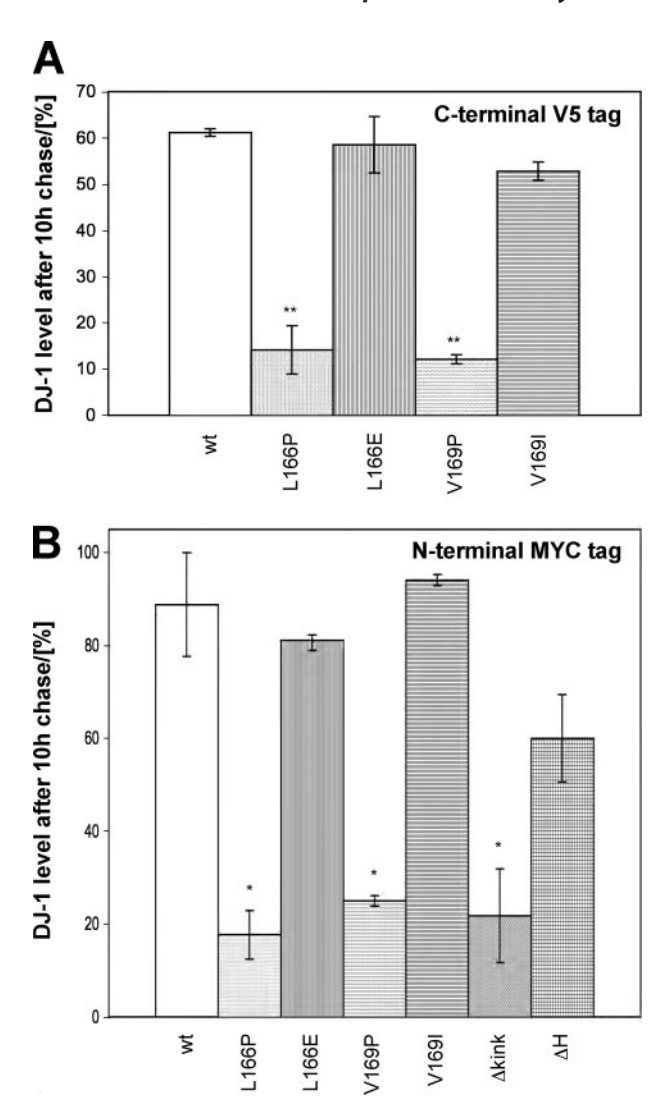


FIGURE 4. **G-helix breaking and kink deletion mutations accelerate degradation of DJ-1 protein.** HEK293T cells were transiently transfected with C-terminal V5-tagged (A) and N-terminal MYC-tagged (B) DJ-1 and the indicated mutants. After a 3-h pulse metabolic labeling with a mixture of [ $^{35}$ S]methionine and [ $^{35}$ S]cysteine, cells were chased with non-radioactive sulfur-containing amino acids. After lysis, DJ-1 proteins were immunoprecipitated with anti-V5 (A) or anti-MYC (B) and subjected to denaturing 15% PAGE. Full-length DJ-1 protein band intensities at the 10-h chase time were quantified with a Phosphorlmager, and expressed as percentage relative to the 0-h time point. Results are mean values of three independent experiments with *error bars* indicating S.E. (A) and two independent experiments with *error bars* indicating range (B). \*, P < 0.05; \*\*\*, P < 0.01; P test.

be rapidly turned over by the proteasome (31), begins to accumulate already by 2 h of epoxomicin exposure. Thus, G-helix disrupting mutations appear to cause a complex DJ-1 breakdown process involving partly the proteasome.

To examine the effects of C-terminal point mutations on the functionally relevant dimer formation of DJ-1 (20 –22), we have co-transfected N-terminal MYC-tagged [wt]DJ-1 with C-terminal V5-tagged DJ-1 constructs harboring severely destabilizing (L166P and V169P) and barely destabilizing (L166E and V169I) mutations in the G-helix. Cells were lysed and mt DJ-1 immunoprecipitated with anti-V5. In contrast to [wt]DJ-1/V5, the steady-state expression of [L166P]DJ-1/V5 and [V169I]DJ-1/V5 were below detection limits on straight Western blots, but the signal could be enriched by immunoprecipitation. Still,

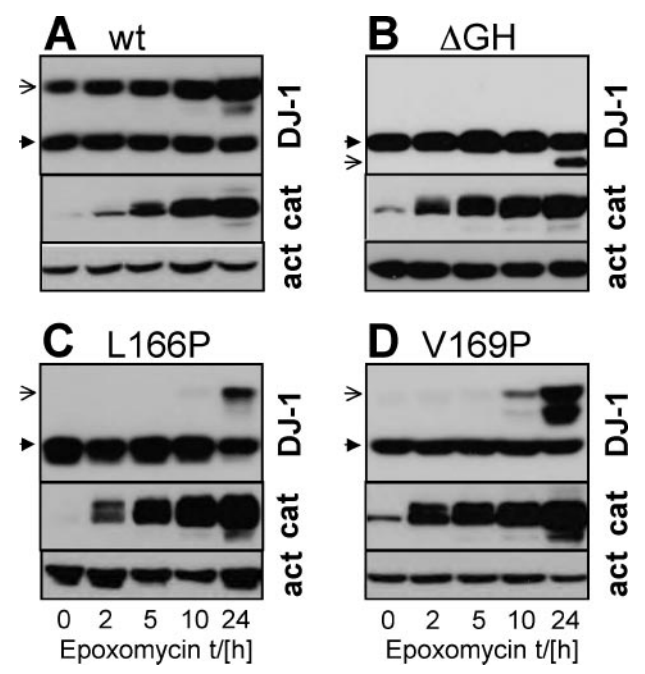


FIGURE 5. **G-helix disrupting DJ-1 mutants are inefficiently stabilized by proteasome inhibition.** HEK293T cells were transiently transfected with [wt]DJ-1/V5 (A), [ $\Delta$ GH]DJ-1/V5 (B), [L166P]DJ-1/V5 (C), and [V169P]DJ-1/V5 (D). After 24 h, cells were harvested immediately or incubated for another 2, 5, 10, and 24 h in the presence of 1  $\mu$ M epoxomicin. After the indicated times, cells were lysed and subjected to denaturing 15% PAGE. Western blots were prepared and sequentially probed with 3407 polyclonal antibody against DJ-1 (top panels), and monoclonal antibodies against  $\beta$ -catenin (middle panels) and  $\beta$ -actin (bottom panels). Endogenous DJ-1 bands are denoted by closed arrows and transfected tagged DJ-1 bands by open arrows. These results are representative for two to three independent experiments.

both the PD-associated [L166P]DJ-1/V5 and our synthetic [V169P]DJ-1/V5 failed to co-immunoprecipitate co-transfected MYC-[wt]DJ-1 (Fig. 6A). In contrast, [wt]DJ-1/V5 as well as the control mutants [L166E]DJ-1/V5 and [V169I]DJ-1/V5 did form heterodimers with the co-transfected MYC/DJ-1.

To examine the influence of deletions within the helix-kinkhelix motif, N-terminal MYC-tagged deletion constructs were co-transfected with [wt]DJ-1/V5 in HEK293T cells, and immunoprecipitated with anti-MYC-agarose conjugate. MYC/ [wt]DJ-1 co-immunoprecipitated with [wt]DJ-1/V5, consistent with the reverse immunoprecipitation above (Fig. 6). The relatively stable MYC/[ $\Delta$ H]DJ-1 was found to co-immunoprecipitate with [wt]DJ-1/V5, whereas the MYC/[ $\Delta$ GH]DJ-1 mutant did not (Fig. 6*B*). Thus, the C-terminal helix-kink-helix motif of DJ-1 is essential for protein stability and dimerization, with relatively little contribution of the H-helix. Interestingly, the destabilizing kink deletion did not abolish heterodimerization with co-transfected [wt]DJ-1/V5 (Fig. 6*B*), suggesting some stabilizing effect of wt DJ-1 homomers.

To test if the reduced stability of mt DJ-1 has functional consequences, and to gain further insight into the physiological role of DJ-1, we investigated cytoprotective effects against  $\rm H_2O_2$  (9). To minimize the strong protective contribution of endogenous DJ-1, which is expressed in quite high amounts in model cell lines (see Fig. 2), we established immortalized MEF cultures from DJ-1 ko mouse embryos. We made use of a peptide antibody (Alphagenix, Inc.) that reacted well with mouse DJ-1 to prove that the relatively low amount of endogenous

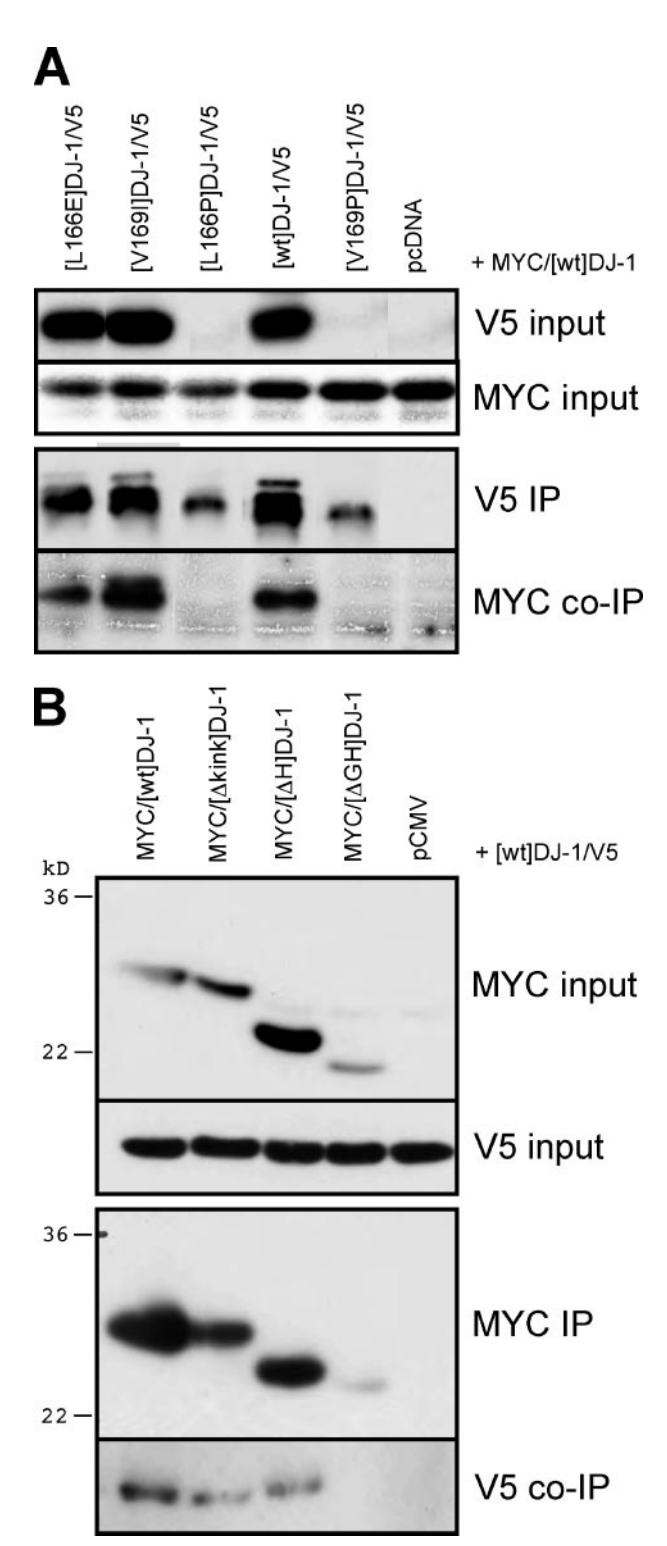


FIGURE 6. DJ-1 dimer formation depends on an intact G-helix. HEK293T cells were co-transfected with MYC/[wt]DJ-1 and the indicated G-helix point mt DJ-1/V5 constructs (A) or [wt]DJ-1/V5 and the indicated MYC/DJ-1 deletion constructs (B). One day after transfection, cells were lysed and (input) directly Western probed with monoclonal antibodies against the MYC and V5 tags, as indicated to the right. Equal amounts of the prey [wt]DJ-1 proteins were detected in the lower input panels. A, monoclonal anti-V5 immunoprecipitates (V5 IP) were Western blotted and probed with anti-V5 (upper panel) as control and with polyclonal anti-MYC (lower panel) to detect co-immunoprecipitation. B, anti-MYC agarosebound proteins were Western blotted and probed with monoclonal anti-MYC (upper panel) as control and with monoclonal anti-V5 (lower panel) to detect coimmunoprecipitation. Positions of molecular weight standards are indicated to the left. The experiment was repeated with the same result.

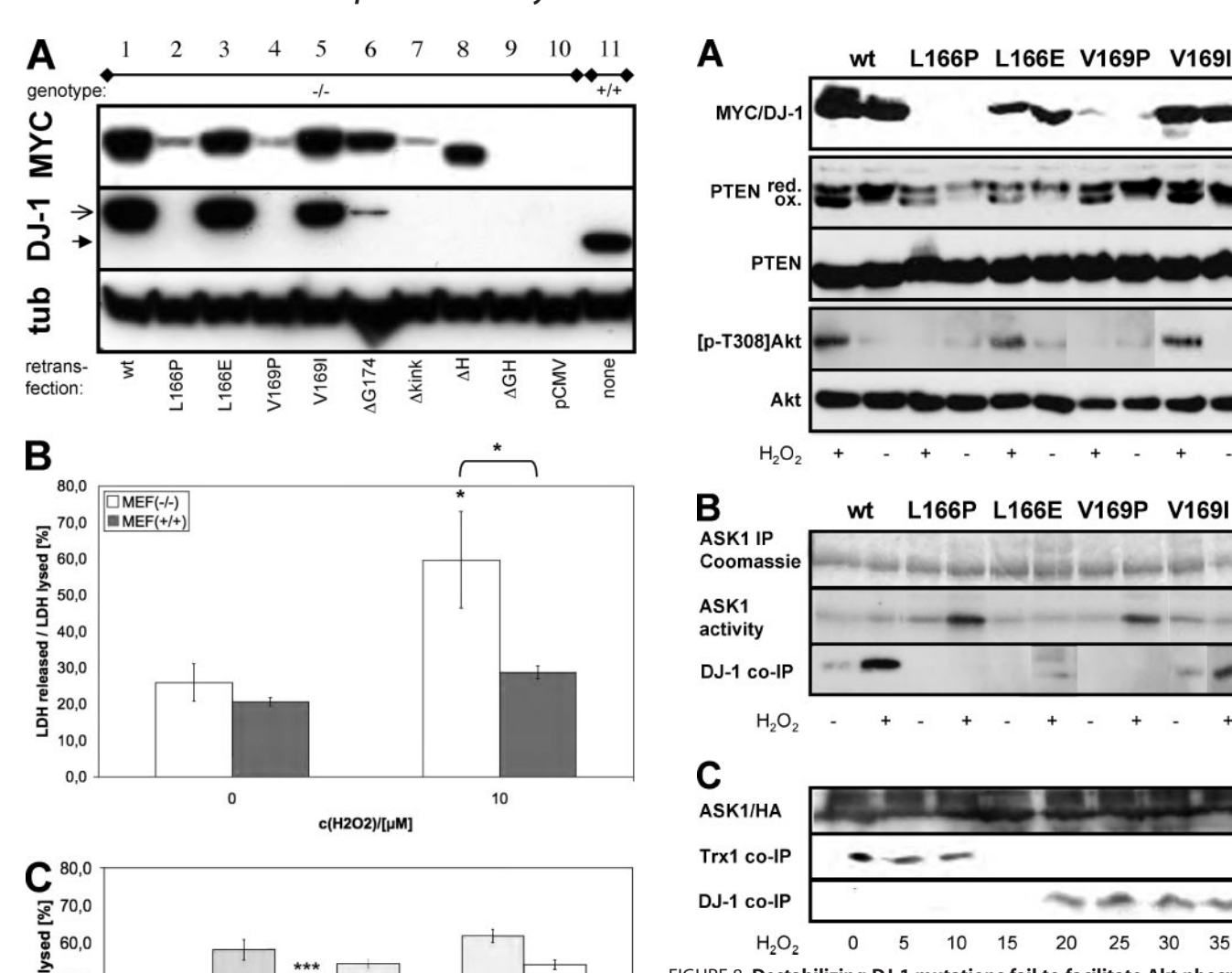
DJ-1 in wt MEFs was completely absent in DJ- $1^{-/-}$  cells (Fig. 7A). These ko cells allow strong and exclusive expression of back-transfected DJ-1. Consistent with the results in HEK293T and PC12 cells (Fig. 2), steady-state levels of [L166E]DJ-1 and [V169I]DJ-1 were similar to those of [wt]DJ-1, whereas MYC/ [L166P]DJ-1 and MYC/[V169P]DJ-1 levels were greatly reduced, and MYC/ $[\Delta GH]DJ$ -1 expression was completely abolished (Fig. 7*A*). In contrast, MYC/[ $\Delta$ H]DJ-1 was detectable practically at wt level with antibodies against the N-terminal MYC tag, whereas the C-terminal epitope recognized by the DJ-1 peptide antibody was deleted (Fig. 7A). Point deletion of the absolutely conserved Gly<sup>174</sup> within the kink reduced MYC/  $[\Delta G174] DJ\text{--}1$  expression in MEF cells, and deletion of both kink amino acids (Asn<sup>173</sup>-Gly<sup>174</sup>) even further reduced MYC/  $[\Delta kink]DJ-1$  steady-state expression to barely detectable levels (Fig. 7A).

DJ-1 ko sensitized MEFs to H<sub>2</sub>O<sub>2</sub> toxicity. LDH release assays revealed that application of 10  $\mu$ M H<sub>2</sub>O<sub>2</sub> for 15 h caused strong cytotoxicity in DJ-1<sup>-/-</sup> MEF cell cultures, whereas DJ-1<sup>+/+</sup> MEFs were refractory to H<sub>2</sub>O<sub>2</sub> toxicity under these conditions (Fig. 7B). Transient re-transfection of DJ-1<sup>-/-</sup> MEFs with [wt]DJ-1 reduced LDH release by 20  $\mu$ M H<sub>2</sub>O<sub>2</sub> by  $\sim$ 50% relative to vector controls, whereas [L166P]DJ-1 and [V169P]DJ-1 had no significant cytoprotective effect (Fig. 7C). The less destabilized [L166E]DJ-1 was fairly cytoprotective, and the stable [V169I]DJ-1 had almost wt survival promoting activity. Like the G-helix incompatible mutants, the unstable kink mutant MYC/ [ $\Delta$ G174]DJ-1 displayed very little cytoprotective activity against  $H_2O_2$  (Fig. 7C). Thus, the destabilizing influence of DJ-1 G-helix breaking and kink perturbing mutations has functional consequences, namely loss of cellular antioxidative defense capacity.

DJ-1 could act as a direct antioxidant (9) or an oxidationactivated chaperone (32, 33). Alternatively, DJ-1 may indirectly mediate cellular survival by facilitating the cytoprotective Akt pathway (14, 15) and/or suppress the pro-apoptotic ASK1 (16). To evaluate the influence of DJ-1 protein destabilizing mutations on these pathways, we transiently transfected DJ-1<sup>-/-</sup> MEF cells with N-terminal MYC-tagged [wt]DJ-1 as well as destabilizing and control mutants in the G-helix.

First we investigated the effects of DJ-1 on PTEN-mediated Akt signaling. We found no yeast two-hybrid interaction and we could not reliably co-immunoprecipitate PTEN and DJ-1 (results not shown), arguing against a stable physical interaction of PTEN and DJ-1. Next, we considered the possibility that DJ-1 modulates the redox activation of PTEN. PTEN is a phosphatase with catalytical cysteine residues that are oxidizable (34). Active (reduced) PTEN can be distinguished from inactive (oxidized) PTEN in a biochemical reaction with NEM (35). The sulfhydryl groups in the catalytic center of PTEN can react with NEM in the free (-SH) but not the oxidized (-SO<sub>n</sub>) state. PTEN-NEM adducts derived from active PTEN migrate slower in SDS-PAGE than inactive PTEN-SO<sub>n</sub>. As shown in Fig. 8A, PTEN in untreated cells was mostly in the active, reduced state, because all of the PTEN immunoreactivity was converted to the NEM-shifted band. After treatment with 500  $\mu$ M H<sub>2</sub>O<sub>2</sub> for 30 min, about half of the PTEN protein failed to react with NEM, indicating oxidation of the reactive sulfhydryl groups. Expres-





40.0 transfected with the MYC/DJ-1 constructs indicated on top, and 48 h later treated (+) or not (-) with 500  $\mu$ M H<sub>2</sub>O<sub>2</sub> for 30 min. A, cell lysates were reacted 30,0 with NEM for 15 min on ice. For PTEN detection, sample aliquots were subjected to denaturing 10% PAGE, omitting the reducing agent dithiothreitol 20,0 for separation of oxidized (lower band) and reduced (upper band) PTEN (second panel). Denaturing 15% PAGE was done for Western probing with 9E10 10,0 anti-MYC to detect tagged DJ-1, as well as total PTEN and phosphorylated and total Akt, as indicated to the left. B, further aliquots of the same lysates 0,0 L166P L166E V169P V169I ΔG174 were immunoprecipitated with anti-ASK1 and stained with Coomassie Blue (upper panel). Immunocomplex ASK1 assays were performed, and incorpora-FIGURE 7. Expression of DJ-1 mutants in MEFs influences cytotoxicity in the presence of  $H_2O_2$ . A, immortalized DJ-1<sup>-/-</sup> MEF cell cultures (lanes 1–10) tion of <sup>32</sup>PO<sub>4</sub> into the substrate myelin basic protein detected by autoradiography (middle panel). DJ-1 co-immunoprecipitated with ASK1 was detected were transiently transfected with the indicated MYC/DJ-1 constructs (lanes on parallel immunoblots probed with 3E8 monoclonal antibody against DJ-1 1-9) or empty vector (*lane 10*). An untransfected wt DJ-1<sup>+/+</sup> control was run in parallel (lane 11). Cell lysates were electrophoresed and Western blots (lower panel). C, HEK293E cells were co-transfected with ASK1/HA and MYC/ DJ-1. After 48 h, cells were exposed to 1000  $\mu$ M H<sub>2</sub>O<sub>2</sub> for the indicated times sequentially probed with antibodies against the MYC tag (top panel) and DJ-1 and lysed. ASK1 complexes were immunoprecipitated with anti-HA-agarose peptide (middle panel). The open arrow points to tagged, transfected DJ-1 and and subjected to 4-20% PAGE. Western blots were sequentially probed with the filled arrow identifies endogenous DJ-1 in wt MEFs. Reprobing the blot for anti-ASK1 (top panel), anti-Trx1 (middle panel), and 9E10 anti-MYC (lower  $\alpha$ -tubulin confirmed equal loading (bottom panel). B, DJ-1<sup>-/</sup> and littermate wt control DJ-1 $^{+/+}$  MEF cell cultures were exposed for 15 h to 0 and 10  $\mu$ M panel). This experiment is representative of three independently repeated experiments.  $H_2O_2$ . Cytotoxicity was determined in LDH release assays. DJ-1<sup>-/-</sup> MEFs were significantly sensitized to H<sub>2</sub>O<sub>2</sub> toxicity. C, DJ-1<sup>-/-</sup> MEFs were transiently

H2O2

sion of DJ-1 did not influence PTEN oxidation in basal and oxidative conditions (Fig. 8A). Thus, DJ-1 does not directly influence the redox state of PTEN. Likewise, global ROS production stimulated by the thiol-selective oxidant diamide (36)

transfected with the indicated MYC/DJ-1 constructs or empty vector. After 2 days, cells were exposed to 20  $\mu$ M H<sub>2</sub>O<sub>2</sub> for 15 h, and cytotoxicity measured as

LDH release. Error bars delineate standard deviation of quadruplicate meas-

urements; \*, p < 0.05; \*\*\*, p < 0.001, t test. The experiment was repeated

another 3 times with DJ-1/V5 constructs yielding the same result.

was not guenched after transfection with any of the MYC/DJ-1 constructs tested (Table 1). In conclusion, DJ-1 does not seem to exert its cytoprotective role as a direct antioxidative agent, but may rather indirectly influence cellular viability redox signaling pathways.

The major redox signaling effector of PTEN (37), Akt was activated upon H<sub>2</sub>O<sub>2</sub> treatment of MYC/[wt]DJ-1-transfected MEF cells, as determined on Western blots using the phospho-

60,0

50,0

ased / LDH

ē

20

25

30

35

10

lation and do not repress ASK1. A and B, immortalized DJ-1

FIGURE 8. Destabilizing DJ-1 mutations fail to facilitate Akt phosphory-

15

#### TABLE 1 ROS production induced by diamide is not guenched by DJ-1

DJ-1<sup>-/-</sup> MEF cells were transiently transfected with N-terminal MYC-tagged DJ-1 constructs harboring the indicated mutations. Cells were loaded with the probe dichlorodihydrofluorescein diacetate, and exposed for 1 h to medium alone or 200 μΜ diamide. ROS production was measured as dichlorofluorescein fluorescence relative to total protein content. Values are mean  $\pm$  S.D. of triplicate measurements.

| Construct     | ROS/relative fluorescence units |                |                |
|---------------|---------------------------------|----------------|----------------|
|               | Control                         | 200 μM Diamide | ROS production |
|               |                                 |                | -fold          |
| pCMV          | $53 \pm 9$                      | $162 \pm 10$   | 3.1            |
| wt            | $60 \pm 8$                      | $228 \pm 21$   | 3.8            |
| L166P         | $53 \pm 6$                      | $160 \pm 26$   | 3.0            |
| L166E         | $55 \pm 8$                      | $163 \pm 13$   | 3.0            |
| V169P         | $65 \pm 9$                      | $239 \pm 7$    | 3.7            |
| V169I         | $50 \pm 8$                      | $164 \pm 11$   | 3.3            |
| $\Delta G174$ | $52 \pm 5$                      | $171 \pm 19$   | 3.3            |

specific [p-T308]Akt antibody. The same strong Akt phosphorylation was observed in H2O2-treated MEF cells transfected with the non-destabilizing MYC/[L166E]DJ-1 and MYC/ [V169I]DJ-1. In sharp contrast, transfection with MYC/ [L166P]DJ-1 and MYC/[V169P]DJ-1 caused a greatly reduced Akt phosphorylation at Thr<sup>308</sup> upon H<sub>2</sub>O<sub>2</sub> treatment, despite constant levels of total Akt (Fig. 8A). Thus, it appears that failure to facilitate the Akt pathway is a common feature of destabilizing, G-helix breaking DJ-1 mutants.

To evaluate the influence of DJ-1 on the pro-apoptotic ASK1 pathway (16), we immunoprecipitated endogenous ASK1 and performed immunocomplex kinase assays using myelin basic protein as substrate. We found no H<sub>2</sub>O<sub>2</sub>-mediated stimulation of ASK1 activity in DJ-1 ko MEF cells transfected with MYC/ [wt]DJ-1 and the control mutants MYC/[L166E]DJ-1 and MYC/[V169I]DJ-1. In contrast, transfection with the PD mutant MYC/[L166P]DJ-1 as well as MYC/[V169P]DJ-1 was permissive for stimulation of ASK1 upon H<sub>2</sub>O<sub>2</sub> treatment (Fig. 8B), consistent with the lack of cytoprotective activity of these G-helix breaking DJ-1 mutants.

Interestingly, anti-ASK1 co-immunoprecipitated MYC/ [wt]DJ-1, and this interaction was greatly increased after  $H_2O_2$ treatment (Fig. 8B). Oxidation-enhanced interaction with ASK1 was also seen for control mutants MYC/[L166E]DJ-1 and MYC/[V169I]DJ-1. In contrast, no co-immunoprecipitation was observed for MYC/[L166P]DJ-1 and MYC/[V169P]DJ-1, even after H2O2 treatment, and these immunocomplexes did show ASK1 activity (Fig. 8B). These results suggest that oxidative stress activates DJ-1 to directly bind ASK1 and inhibit the pro-apoptotic ASK1 pathway.

ASK1 activity is normally suppressed by binding to reduced Trx1, and ROS production causes dissociation of oxidized Trx1 and activation of the ASK1 signalosome (38 – 40). To test if the redox-sensitive DJ-1 had a similar effect on ASK1, we co-immunoprecipitated HA-tagged ASK1 with endogenous Trx1 and co-transfected MYC/DJ-1. In control HEK293E cells, ASK1/HA co-immunoprecipitated with Trx1, but not with MYC/DJ-1 (Fig. 8C). After a 15-min H<sub>2</sub>O<sub>2</sub> treatment, Trx1 dissociated from ASK1/HA (Fig. 8C). Interestingly, MYC/DJ-1 binding to ASK1/HA followed Trx1 dissociation after a 20-min H<sub>2</sub>O<sub>2</sub> challenge (Fig. 8C). Thus, Trx1 and DJ-1 sequentially bind to ASK1 and thus might both contribute to suppression of ASK1 activity under acute oxidative stress.

#### DISCUSSION

Several sometimes conflicting findings about DJ-1 activities have been reported, including oncogenesis, RNA binding, male fertility, transcriptional modulation, molecular chaperoning, and management of oxidative stress (7, 9, 11, 15, 25, 32, 33, 41–50). However, the molecular mechanisms and cellular roles of the ubiquitously expressed and evolutionarily extremely conserved DJ-1 remain unclear, and particularly how loss of DJ-1 causes PD is not understood.

Solving the crystal structure of DJ-1 and related proteins has prompted a number of rational hypotheses about DJ-1 functions. DJ-1 proteins are structurally similar to bacterial PH1704-type proteases (23, 24, 26, 27). However, the putative active site with Cys<sup>106</sup> as potential catalytic residue and His<sup>126</sup> is missing an acidic residue (glutamate in PH1704) to complete the catalytic triad of this class of proteases. Moreover, the putative DJ-1 active site is occluded by the C-terminal helix-kinkhelix motif. There is little experimental evidence that DJ-1 acts as a protease.

Structural similarity to Hsp31 suggested some chaperone activity of DJ-1 (25), although the helix-sheet-helix sandwich structure that characterizes the DJ-1 superfamily actually forms a domain outside the catalytic center of Hsp31. In vitro chaperone activity of DJ-1 toward  $\alpha$ -synuclein, the major misfolded protein in PD and related diseases was shown to depend on oxidative conditions (32, 33). It remains to be confirmed in vivo that DJ-1 has direct chaperone activity.

It is remarkable that the tertiary structure of DJ-1 differs from all other members of this protein superfamily by the presence of a C-terminal helix-kink-helix motif. Importantly, the most deleterious DJ-1 point mutation, L166P, resides in this C-terminal motif. To investigate structural determinants of the helix-kink-helix motif, we have performed an extensive mutagenesis study. Introduction of helix-breaking proline residues in the G-helix (both PD-associated L166P and our synthetic V169P one helical turn downstream) resulted in dramatically destabilized DJ-1 mutants. Although the amounts of immunoprecipitated G-helix breaking and deletion mutants were relatively low, our co-immunoprecipitation experiments indicated that the quarternary structure of DJ-1 was disrupted by G-helix breaking mutations, consistent with the rather large surface of the DJ-1 C terminus that forms part of the dimer interface. By comparison, hydrophobic side chains pointing into the helix-kink-helix motif, and the H-helix turned out to be of lesser importance for DJ-1 stability.

Perhaps less expectedly, the sharp kink between helices G and H was found to be an important determinant for DJ-1 protein stability. Kink deletions destabilized the DJ-1 protein (Fig. 2, *B* and *D*), and point deletion of the absolutely conserved tight turn Gly<sup>174</sup> was found to be sufficient for this effect in DJ-1<sup>-/-</sup> MEF cells devoid of endogenous [wt]DJ-1 (Fig. 7A). MYC/ [ $\Delta$ kink]DJ-1 retained some capacity to form heterodimers with co-transfected [wt]DJ-1/V5 (Fig. 6B), in contrast to mutant homodimers that were undetectable (results not shown). Although the low expression levels of destabilized DJ-1 mutants make it difficult to distinguish loss-of-function from simple loss-of-protein, our experiments support the view that



dimerization is crucial for DJ-1 stability in a recessive manner, consistent with the recessive association of DJ-1 with PD (1). We conclude that the DJ-1 dimer is a globular protein with the PD-associated L166P mutant containing helix G and kink as critical determinant and lesser contribution of helix H. Our study shows that the unique DJ-1 helix-kink-helix motif is not an independent domain but an integral part of functional, stable DJ-1 dimers.

Previous studies had implicated the proteasome in [L166P]DJ-1 degradation, although full recovery was not achieved with proteasome inhibitors (17, 20–22). In accord with our previous studies (17), the reversible proteasome inhibitor MG-132 failed to stabilize our new synthetic mutants. However, the more specific, irreversible proteasome inhibitor epoxomicin caused some accumulation of [L166P]DJ-1/V5 as well as [V169P]DJ-1/V5 and [ $\Delta$ GH]DJ-1/V5, but only after long-term treatment, and wt levels were mostly not reached even under these conditions. Thus, degradation of unstable DJ-1 mutants is a complex process that involves in part the proteasome.

To demonstrate that the destabilizing DJ-1 mutations caused functional impairments, we established a cell culture system in which no endogenous DJ-1 obscures any effects of loss-of-function DJ-1 mutants. MEF cells were derived from DJ-1 $^{-/-}$  mouse embryos and immortalized with the large T oncogene. As expected, compared with DJ-1 $^{+/+}$  littermate control MEFs, our DJ-1 $^{-/-}$  MEFs were sensitized to  $\rm H_2O_2$  toxicity. In these cells, steady-state levels of transiently transfected [L166P]DJ-1, [V169P]DJ-1, and [ $\Delta G174$ ]DJ-1 were dramatically reduced compared with [wt]DJ-1 and the control mutants [L166E]DJ-1 and [V169I]DJ-1. Consistently, the destabilizing mutants lost cytoprotective activity against  $\rm H_2O_2$  (Fig. 7).

Although DJ-1 appears to have limited direct antioxidative activity (9), the effect seems to be quite weak to explain the powerful cytoprotective functions of DJ-1. When determining the highly sensitive redox state of PTEN (35), we found that DJ-1 failed to exert Trx activity on PTEN in H<sub>2</sub>O<sub>2</sub>-exposed MEF cells. Global ROS production induced by diamide was also not reduced by DJ-1. Thus, DJ-1 may not be a major antioxidative enzyme itself, but play a role as redox sensor that regulates signaling cascades protecting cells against oxidative stress. Here we show that DJ-1 concomitantly facilitates the survivalpromoting Akt pathway and suppresses the pro-apoptotic ASK1 (Fig. 8). We demonstrate that DJ-1 co-immunoprecipitates with ASK1 upon H<sub>2</sub>O<sub>2</sub> exposure. Interestingly, DJ-1 appeared to bind to ASK1 after dissociation of Trx1, which normally binds to ASK1 in an inhibitory manner (40). It is possible that DJ-1 replaces Trx1 under acute oxidative stress, providing a second safeguard suppressing ASK1-mediated apoptosis. Our results indicate that DJ-1 mediates its effects on ASK1 directly and not (only) via the indirect mechanism of nuclear Daxx sequestration as proposed by Junn et al. (16).

The great majority of the highly soluble wt DJ-1 protein is in the cytosol, and we suggest that a pivotal role of DJ-1 is to react with ROS in the vicinity of mitochondria and throughout the cytoplasm. Under these conditions, DJ-1 directly binds to and inhibits the pro-apoptotic ASK1, and at the same time facilitates the Akt pathway, which among many effectors suppresses

apoptotic genes (37). It will be interesting to study how DJ-1 is involved in transcriptional regulation of Akt target genes.

DJ-1 might act cell autonomously to block ASK1 and facilitate Akt in stressed dopaminergic neurons. PD mutations in humans as well as targeted disruption of DJ-1 in mice and flies do not cause acute cell loss. Dopaminergic neurodegenerative phenotypes only become apparent under stress conditions in DJ-1 ko flies and mice (10, 13, 14). Basal morphology and viability/growth properties of our DJ-1 ko MEF cell cultures did not differ from DJ-1 wt MEFs (Fig. 7B). Thus, DJ-1 appears to be part of a redundant signaling network that becomes active upon oxidative stress. This could even involve trans-cellular mechanisms. Reactive astrocytes greatly up-regulate DJ-1 in chronic and acute neurodegenerative diseases (2-4). DJ-1 was recently found to regulate antioxidant transcriptional responses leading to induction of glutathione biosynthesis and expression of extracellular superoxide dismutase in cell lines (50-52). Although it remains to be confirmed that astrocytes proper are capable of DJ-1-regulated induction of antioxidative genes, it is known that astrocytes support adjacent, stressed neurons with secreted glutathione precursors and secreted superoxide dismutase (5). Therefore, loss-of-function mutations disrupting the unique C-terminal helix-kink-helix motif of DJ-1 probably weaken anti-oxidative defense pathways in cells and organs, most prominently the PD-affected nigral dopaminergic neurons with their high basal oxidative burden. It will be interesting to study if and how the DJ-1 inhibition of ASK1 breaks down in PD, and if the DJ-1-ASK1 complex might be exploited as a novel drug target for neurodegenerative diseases and other age-related disorders.

Acknowledgments—We thank Hubert Kettenberger for advice on molecular modeling, Ben Vanmassenhove for quantitative reverse transcriptase-PCR advice, and Manuela Neumann and Hans Kretzschmar for access to the LightCycler, Paul Saftig for MEF cell culture advice and the donation of large T plasmid, Stephen Hall for the generous donation of antibodies, Hidenori Ichijo for providing ASK1 constructs and antibodies, Wolfdieter Springer for help with the yeast two-hybrid system, Anja Capell, Susanne Schöbel, Stefan Lichtenthaler, and Harald Steiner for helpful discussions, and Thomas Gasser for support.

#### REFERENCES

- Bonifati, V., Rizzu, P., van Baren, M. J., Schaap, O., Breedveld, G. J., Krieger, E., Dekker, M. C. J., Squitieri, F., Ibanez, P., Joosse, M., van Dongen, J. W., Vanacore, N., van Swieten, J. C., Brice, A., Meco, G., van Duijn, C. M., Oostra, B. A., and Heutink, P. (2003) Science 299, 256–259
- Bandopadhyay, R., Kingsbury, A. E., Cookson, M. R., Reid, A. R., Evans, I. M., Hope, A. D., Pittman, A. M., Lashley, T., Canet-Avilés, R., Miller, D. W., McLendon, C., Strand, C., Leonard, A. J., Abou-Sleiman, P. M., Healy, D. G., Ariga, H., Wood, N. W., de Silva, R., Revesz, T., Hardy, J. A., and Lees, A. J. (2004) *Brain* 127, 420 430
- Neumann, M., Müller, V., Görner, K., Kretzschmar, H. A., Haass, C., and Kahle, P. J. (2004) Acta Neuropathol. 107, 489 – 496
- 4. Rizzu, P., Hinkle, D. A., Zhukareva, V., Bonifati, V., Severijnen, L.-A., Martinez, D., Ravid, R., Kamphorst, W., Eberwine, J. H., Lee, V. M.-Y., Trojanowski, J. Q., and Heutink, P. (2004) *Ann. Neurol.* **55**, 113–118
- Heales, S. J. R., Lam, A. A. J., Duncan, A. J., and Land, J. M. (2004) Neurochem. Res. 29, 513–519
- 6. Choi, J., Sullards, M. C., Olzmann, J. A., Rees, H. D., Weintraub, S. T.,



- Bostwick, D. E., Gearing, M., Levey, A. I., Chin, L.-S., and Li, L. (2006) J. Biol. Chem. 281, 10816-10824
- 7. Canet-Avilés, R. M., Wilson, M. A., Miller, D. W., Ahmad, R., McLendon, C., Bandyopadhyay, S., Baptista, M. J., Ringe, D., Petsko, G. A., and Cookson, M. R. (2004) Proc. Natl. Acad. Sci. U. S. A. 101, 9103-9108
- 8. Ooe, H., Taira, T., Iguchi-Ariga, S. M. M., and Ariga, H. (2005) Toxicol. Sci. 88, 114-126
- 9. Taira, T., Saito, Y., Niki, T., Iguchi-Ariga, S. M. M., Takahashi, K., and Ariga, H. (2004) EMBO Rep. 5, 213-218
- 10. Kim, R. H., Smith, P. D., Aleyasin, H., Hayley, S., Mount, M. P., Pownall, S., Wakeham, A., You-Ten, A. J., Kalia, S. K., Horne, P., Westaway, D., Lozano, A. M., Anisman, H., Park, D. S., and Mak, T. W. (2005) Proc. Natl. Acad. Sci. U. S. A. 102, 5215–5220
- 11. Martinat, C., Shendelman, S., Jonason, A., Leete, T., Beal, M. F., Yang, L., Floss, T., and Abeliovich, A. (2004) PLoS Biol. 2, e327
- 12. Menzies, F. M., Yenisetti, S. C., and Min, K.-T. (2005) Curr. Biol. 15,
- 13. Meulener, M., Whitworth, A. J., Armstrong-Gold, C. E., Rizzu, P., Heutink, P., Wes, P. D., Pallanck, L. J., and Bonini, N. M. (2005) Curr. Biol. **15,** 1572-1577
- 14. Yang, Y., Gehrke, S., Haque, M. E., Imai, Y., Kosek, J., Yang, L., Beal, M. F., Nishimura, I., Wakamatsu, K., Ito, S., Takahashi, R., and Lu, B. (2005) Proc. Natl. Acad. Sci. U. S. A. 102, 13670-13675
- 15. Kim, R. H., Peters, M., Jang, Y., Shi, W., Pintilie, M., Fletcher, G. C., De-Luca, C., Liepa, J., Zhou, L., Snow, B., Binari, R. C., Manoukian, A. S., Bray, M. R., Liu, F.-F., Tsao, M. S., and Mak, T. W. (2005) Cancer Cell 7, 263-273
- 16. Junn, E., Taniguchi, H., Jeong, B. S., Zhao, X., Ichijo, H., and Mouradian, M. M. (2005) Proc. Natl. Acad. Sci. U. S. A. 102, 9691–9696
- 17. Görner, K., Holtorf, E., Odoy, S., Nuscher, B., Yamamoto, A., Regula, J. T., Beyer, K., Haass, C., and Kahle, P. J. (2004) J. Biol. Chem. 279, 6943-6951
- 18. Lockhart, P. J., Lincoln, S., Hulihan, M., Kachergus, J., Wilkes, K., Bisceglio, G., Mash, D. C., and Farrer, M. J. (2004) J. Med. Genet. 41, e22
- 19. Macedo, M. G., Anar, B., Bronner, I. F., Cannella, M., Squitieri, F., Bonifati, V., Hoogeveen, A., Heutink, P., and Rizzu, P. (2003) Hum. Mol. Genet. 12,
- 20. Miller, D. W., Ahmad, R., Hague, S., Baptista, M. J., Canet-Avilés, R., McLendon, C., Carter, D. M., Zhu, P.-P., Stadler, J., Chandran, J., Klinefelter, G. R., Blackstone, C., and Cookson, M. R. (2003) J. Biol. Chem. 278, 36588 - 36595
- 21. Moore, D. J., Zhang, L., Dawson, T. M., and Dawson, V. L. (2003) J. Neurochem. 87, 1558-1567
- 22. Olzmann, J. A., Brown, K., Wilkinson, K. D., Rees, H. D., Huai, Q., Ke, H., Levey, A. I., Li, L., and Chin, L.-S. (2004) J. Biol. Chem. 279, 8506 – 8515
- 23. Honbou, K., Suzuki, N. N., Horiuchi, M., Niki, T., Taira, T., Ariga, H., and Inagaki, F. (2003) J. Biol. Chem. 278, 31380-31384
- 24. Huai, Q., Sun, Y., Wang, H., Chin, L.-S., Li, L., Robinson, H., and Ke, H. (2003) FEBS Lett. 549, 171–175
- 25. Lee, S.-J., Kim, S. J., Kim, I.-K., Ko, J., Jeong, C.-S., Kim, G.-H., Park, C., Kang, S.-O., Suh, P.-G., Lee, H.-S., and Cha, S.-S. (2003) J. Biol. Chem. 278, 44552-44559

- 26. Tao, X., and Tong, L. (2003) J. Biol. Chem. 278, 31372-31379
- Wilson, M. A., Collins, J. L., Hod, Y., Ringe, D., and Petsko, G. A. (2003) Proc. Natl. Acad. Sci. U. S. A. 100, 9256-9261
- 28. Wilson, M. A., Ringe, D., and Petsko, G. A. (2005) J. Mol. Biol. 353,
- 29. Bandyopadhyay, S., and Cookson, M. R. (2004) BMC Evol. Biol. 4, 6
- 30. Cookson, M. R. (2003) Proc. Natl. Acad. Sci. U. S. A. 100, 9111–9113
- 31. Aberle, H., Bauer, A., Stappert, J., Kispert, A., and Kemler, R. (1997) EMBO I. 16, 3797-3804
- 32. Shendelman, S., Jonason, A., Martinat, C., Leete, T., and Abeliovich, A. (2004) PLoS Biol. 2, e362
- Zhou, W., Zhu, M., Wilson, M. A., Petsko, G. A., and Fink, A. L. (2006) J. Mol. Biol. 356, 1036-1048
- 34. Leslie, N. R., and Downes, C. P. (2004) Biochem. J. 382, 1-11
- 35. Lee, S.-R., Yang, K.-S., Kwon, J., Lee, C., Jeong, W., and Rhee, S. G. (2002) J. Biol. Chem. 277, 20336-20342
- 36. Kosower, N. S., and Kosower, E. M. (1987) Methods Enzymol. 143, 264 - 270
- 37. Barthel, A., and Klotz, L.-O. (2005) Biol. Chem. 386, 207-216
- 38. Liu, H., Nishitoh, H., Ichijo, H., and Kyriakis, J. M. (2000) Mol. Cell. Biol. 20, 2198 - 2208
- 39. Noguchi, T., Takeda, K., Matsuzawa, A., Saegusa, K., Nakano, H., Gohda, J., Inoue, J., and Ichijo, H. (2005) J. Biol. Chem. 280, 37033-37040
- Saitoh, M., Nishitoh, H., Fujii, M., Takeda, K., Tobiume, K., Sawada, Y., Kawabata, M., Miyazono, K., and Ichijo, H. (1998) EMBO J. 17, 2596 - 2606
- 41. Hod, Y., Pentyala, S. N., Whyard, T. C., and El-Maghrabi, M. R. (1999) J. Cell. Biochem. 72, 435-444
- 42. Li, H. M., Niki, T., Taira, T., Iguchi-Ariga, S. M. M., and Ariga, H. (2005) Free Radic. Res. 39, 1091-1099
- 43. Moore, D. J., Zhang, L., Troncoso, J., Lee, M. K., Hattori, N., Mizuno, Y., Dawson, T. M., and Dawson, V. L. (2005) Hum. Mol. Genet. 14, 71-84
- 44. Nagakubo, D., Taira, T., Kitaura, H., Ikeda, M., Tamai, K., Iguchi-Ariga, S. M. M., and Ariga, H. (1997) Biochem. Biophys. Res. Commun. 231, 509 - 513
- 45. Okada, M., Matsumoto, K., Niki, T., Taira, T., Iguchi-Ariga, S. M. M., and Ariga, H. (2002) Biol. Pharm. Bull. 25, 853-856
- 46. Shinbo, Y., Taira, T., Niki, T., Iguchi-Ariga, S. M. M., and Ariga, H. (2005) Int. J. Oncol. 26, 641-648
- 47. Takahashi, K., Taira, T., Niki, T., Seino, C., Iguchi-Ariga, S. M. M., and Ariga, H. (2001) J. Biol. Chem. 276, 37556-37563
- 48. Wagenfeld, A., Gromoll, J., and Cooper, T. G. (1998) Biochem. Biophys. Res. Commun. 251, 545-549
- 49. Xu, J., Zhong, N., Wang, H., Elias, J. E., Kim, C. Y., Woldman, I., Pifl, C., Gygi, S. P., Geula, C., and Yankner, B. A. (2005) Hum. Mol. Genet. 14, 1231-1241
- 50. Zhou, W., and Freed, C. R. (2005) J. Biol. Chem. 280, 43150 43158
- Clements, C. M., McNally, R. S., Conti, B. J., Mak, T. W., and Ting, J. P.-Y. (2006) Proc. Natl. Acad. Sci. U. S. A. 103, 15091–15096
- 52. Nishinaga, H., Takahashi-Niki, K., Taira, T., Andreadis, A., Iguchi-Ariga, S. M. M., and Ariga, H. (2005) Neurosci. Lett. 390, 54-59



# Supplementary Table: Sequences of Mutagenesis Primers.

| Mutants     | Forward primers                         | Reverse primers                            |
|-------------|---|--|
| [L166P]DJ-1 | 5'-CTTCGAGTTTGCGCCTGCAATTGTTGAA-3'      | 5'-TTCAACAATTGCAGGCGCAAACTCGAAG-3'         |
| [L166E]DJ-1 | 5'-CTTCGAGTTTGCGGAAGCAATTGTTGAA-3'      | 5'-TTCAACAATTGCTTCGGCAAACTCGAAG-3'         |
| [V169P]DJ-1 | 5'-CGCTTGCAATTCCTGAAGCCCTGAA-3'         | 5'-TTCAGGGCTTCAGGAATTGCAAGCG-3'            |
| [V169I]DJ-1 | 5'-CGCTTGCAATTATTGAAGCCCTGAA-3'         | 5'-TTCAGGGCTTCAATAATTGCAAGCG-3'            |
| [V169A]DJ-1 | 5'-GCTTGCAATTGCTGAAGCCCTGAA-3'          | 5'-TTCAGGGCTTCAGCAATTGCAAGC-3'             |
| [ΔG174]DJ-1 | 5'-TTGAAGCCCTGAATAAGGAGGTGGCGG-3'       | 5'-CCGCCACCTCCTTATTCAGGGCTTCAA-3'          |
| [A178P]DJ-1 | 5'-AAGGAGGTGCCGGCTCAAGTGA-3'            | 5'-TCACTTGAGCCGGCACCTCCTT-3'               |
| [V181P]DJ-1 | 5'-GCGGCTCAACCGAAGGCTCCA-3'             | 5'-TGGAGCCTTCGGTTGAGCCGC-3'                |
| [K182P]DJ-1 | 5'-GCTCAAGTGCCGGCTCCACTTGTT-3'          | 5'-AACAAGTGGAGCCGGCACTTGAGC-3'             |
| [L185P]DJ-1 | 5'-TGAAGGCTCCACCTGTTCTTAAAGAC-3'        | 5'-ATCTGGATCCGTCTTTAAGAACAGGTGGAGCCTT-3'   |
| [L187P]DJ-1 | 5'-CTCCACTTGTTCCTAAAGACAAGGG-3'         | 5'-ATCTGGATCCGTCTTTAGGAACAAGTGGAGCCTT-3'   |
| [ΔH]DJ-1    | 5'-CCCGAATTCATGGGAATGGCTTCCAAAAGAGCT-3' | 5'-AAAGCGGCCGCATTCAGGGCTTCAACAATTGCAAGC-3' |
| [Δkink]DJ-1 | 5'-TGTTGAAGCCCTGAAGGAGGTGGC-3'          | 5-ATTGCGGCCGCGTCTTTAAGAACAAGTGGAGCC-3      |
| [ΔGH]DJ-1   | 5'-CCCGAATTCATGGGAATGGCTTCCAAAAGAGCT-3' | 5'-AAAGCGGCCGCGGTCCCAGGCCCCC-3'            |

# Structural Determinants of the C-terminal Helix-Kink-Helix Motif Essential for Protein Stability and Survival Promoting Activity of DJ-1

Karin Görner, Eve Holtorf, Jens Waak, Thu-Trang Pham, Daniela M. Vogt-Weisenhorn, Wolfgang Wurst, Christian Haass and Philipp J. Kahle

J. Biol. Chem. 2007, 282:13680-13691. doi: 10.1074/jbc.M609821200 originally published online March 1, 2007

Access the most updated version of this article at doi: 10.1074/jbc.M609821200

#### Alerts:

- When this article is cited
- · When a correction for this article is posted

Click here to choose from all of JBC's e-mail alerts

# Supplemental material:

http://www.jbc.org/content/suppl/2007/03/06/M609821200.DC1.html

This article cites 52 references, 29 of which can be accessed free at http://www.jbc.org/content/282/18/13680.full.html#ref-list-1